
Research Paper

A Study on the Effect of Wet Granulation on Microcrystalline Cellulose Particle Structure and Performance

Sherif I. Farag Badawy,^{1,2} David B. Gray,¹ and Munir A. Hussain¹

Received August 18, 2005; accepted November 17, 2005

Purpose. The aim of this study was to investigate the mechanism of the effect of wet granulation process on the compaction properties of microcrystalline cellulose (MCC).

Methods. MCC alone and with hydroxypropyl cellulose (HPC) as a binder were wet granulated by a high-shear process using different granulation parameters (over- and undergranulated). Overgranulated batches were also ball milled after drying and compared to the unmilled material. MCC starting material and granulation were characterized for particle size distribution, surface area, porosity, and isothermal moisture uptake. Compaction behavior of the MCC and granulations was also studied using a compaction simulator.

Results. In all cases, the wet granulation process decreased MCC primary particle porosity. Wet granulation also reduced compactibility of MCC to different degrees. Overgranulated batch with HPC showed the lowest compactibility and was less compactible than the batch without HPC granulated using the same parameters. Ball-milled material showed an increase in porosity and was significantly more compactible than the unmilled granulation from the same batch.

Conclusions. The decrease in MCC compactibility after granulation is associated with the decrease in MCC primary particle porosity and in some cases with the formation of large dense granules as well. Under certain conditions, milling seems to counteract the effect of wet granulation on MCC compactibility.

KEY WORDS: compactibility; microcrystalline cellulose; porosity; surface area; wet granulation.

INTRODUCTION

Microcrystalline cellulose (MCC) is a widely used pharmaceutical excipient in the manufacture of solid dosage forms due to its desirable attributes. In particular, MCC has excellent compactibility, which makes it a valuable excipient in the formulation of a tablet dosage form. Partially crystalline cellulose fibrils represent the basic structure component of MCC. Those fibrils agglomerate into fibril aggregates, which are in turn combined to form the particles of commercially available MCC grades (1). It has been recognized that MCC compactibility can be significantly reduced upon wet granulation (2). The mechanism of MCC compactibility loss resulting from wet granulation is not well understood. Several reports have attempted to explain the underlying cause of the effect of wet granulation on MCC compactibility. Nevertheless, there is little consensus among those reports. Many authors suggested a change in the nature of MCC resulting in the decrease in compactibility. Buckton *et al.* (3) suggested a change in the internal bonding within the cellulose upon wet granulation and drying, which produced an altered physical structure and was manifested

by the change in enthalpy of water sorption. The change in the extent of hydrogen bonding between the cellulose hydroxy groups has also been suggested to occur upon wet processing (4,5). Later reports, however, failed to detect significant differences in the degree of hydrogen bonding due to wet granulation and extrusion of MCC (6). Suzuki *et al.* (7) suggested a change in the crystallinity of MCC upon high-shear wet granulation, where the crystallite size of cellulose determined by an X-ray diffraction technique was found to decrease with increasing granulation time and the amount of granulating water. Other authors have suggested a crystallite gel model (8) or a sponge model (9) to describe the performance of MCC during wet processing.

Although the change in the internal structure of MCC suggested by those reports could result in the compactibility changes induced by wet granulation, an alternative scenario can be contemplated. The agglomeration of primary particles of pharmaceutical powder into larger dense granules has been shown to diminish compactibility, even without changes in primary particle structure. The "overgranulation" of lactose using excessive water and shear forces was found to decrease its compactibility upon wet granulation in a high-shear mixer. In this case, the failure of the large dense granules with reduced surface area to significantly fracture or deform upon application of the compression force was shown to result in the decrease in compactibility (10,11). A similar observation was suggested for MCC pellets manufactured by

¹ Pharmaceutical Research Institute, Bristol-Myers Squibb Co., One Squibb Drive, New Brunswick, New Jersey 08903, USA.

² To whom correspondence should be addressed. (e-mail: sherif.badawy@bms.com)

an extrusion/spheronization technique. Tensile strength of compacts formed at a given compression pressure was inversely related to pellet porosity (12). The diminished porosity of MCC granules produced by wet granulation has also been reported by Westermack *et al.* (13).

The aim of this study is to provide further understanding of the behavior of MCC in wet granulation. The relevance of particle and/or granule porosity to compactibility of MCC based formulations is investigated. The porosity changes in MCC upon wet granulation are characterized with an attempt to distinguish between pores within primary MCC particles and those between particles in a granule. The effect of binder addition and subsequent milling of dried granules on MCC compactibility loss is also evaluated. In addition, the effect of wet granulation on MCC lubricant sensitivity is examined.

EXPERIMENTAL

Materials

Microcrystalline cellulose (Emcocel 90M) was obtained from JRS Pharma (Patterson, NY, USA). Hydroxypropyl cellulose (Klucel LF) was supplied by Aqualon (Wilmington, DE, USA), and magnesium stearate was obtained from Mallinckrodt (St. Louis, MO, USA).

Methods

Granulation Batches in the High-Shear Mixer

Three granulation batches of MCC were manufactured by high-shear wet granulation. Two of the batches contained 3% hydroxypropyl cellulose (HPC), whereas the third batch consisted of only MCC. The two batches containing HPC were granulated using two different granulation parameters (overgranulated and undergranulated batches). Formulation without HPC was granulated using identical parameters as the overgranulated batch with HPC.

Granulation of the three batches was carried out in a Key 1L high-shear granulator (Key International, English-town, NJ, USA) using a batch size of 150 g and water as the granulating liquid. Batches containing HPC were manufactured by blending MCC and HPC in the high-shear mixer for 2 min at 500 rpm. For the undergranulated batch with HPC (batch 1), 57 g of water was added to the MCC-HPC mixture in the granulator at a rate of 12 g/minute using a peristaltic pump, with impeller speed maintained at 500 rpm. The wet granulation was wet massed for 30 s after complete addition of water while maintaining the impeller speed at 500 rpm. The wet granulation was dried in a hot-air convection oven at 50°C to a moisture content of NMT 3.5%. Granulation was then screened through 20-mesh screen.

The overgranulated HPC-containing batch (batch 2) was manufactured using 83 g of water, 777 rpm impeller speed, and 4 min wet massing time. Other process steps and parameters were identical to those used with the undergranulated batch (batch 1). For the overgranulated batch without HPC (batch 3), MCC was mixed in the high-shear granulator for 2 min at 777 rpm and then granulated using identical parameters as batch 2.

For the two overgranulated batches, a sample of the dried and screened granulation was ball milled using a Fritsch planetary micromill (Idar-oberstein, Germany). Approximately 10 g sample was placed in the milling jar containing 12 stainless steel balls, 11.9 mm in diameter. The mill was then run for 60 min at 200 rpm.

Lubrication of the granulation was performed by blending the dried and screened granulation with a quantity of magnesium stearate representing 0.5% of the final batch weight in a 1/2-qt V-blender for 10 min.

Physical Characterization of the Granulation and MCC Starting Material

Particle Size Distribution

Particle size distribution of the dried granulation and MCC starting material was determined by mesh analysis using an Allen Bradley Sonic Sifter (Milwaukee, WI, USA) equipped with a series of six screens and a pan. An approximately 5 g sample was tested with a pulse setting of 5, sift setting of 5, and a total sifting time of 5 min. Particle size distribution of the dried granulation and MCC starting material was also determined by a dry laser-diffraction technique (Mastersizer 200, Malvern Instruments Ltd., Malvern, UK).

Porosity Determination by Mercury Intrusion Porosimetry

Pore volume distribution of the granulation and MCC starting material was determined by mercury intrusion porosimetry (MIP; AutoPore III, Micromeritics, Norcross, GA, USA). A sample (0.3–0.5 g) of the particle size fraction passing through 70-mesh screen and retained on 100-mesh screen was used for the porosity determination, except for the ball-milled material. Due to the small particle size of the ball-milled material, it was not possible to collect a 70–100 mesh fraction and hence the whole particle size distribution was used. In all cases, incremental pore volume was determined at different pressures ranging from 1 to 61,000 psi. The pore diameter corresponding to a given pressure was calculated by the software of the instrument according to the Washburn equation (14) using mercury surface tension value of 485 dyn/cm and mercury contact angle of 130°.

Surface Area and Porosity Determination by Nitrogen Adsorption

Surface area and porosity of the granulation and MCC starting material were determined using a nitrogen adsorption technique (Gemini 2380 physisorption analyzer, Micromeritics, Norcross, GA, USA). The sample (1.3–1.5 g) was degassed by nitrogen flow at 60°C for at least 2 h (VacPrep 061, Micromeritics). The amount of nitrogen adsorbed was determined at partial nitrogen vapor pressure (P/P_0) ranging between 0.05 and 0.98. Surface area was determined by the Gemini software using Brunauer, Emmett, and Teller (BET) calculation for the nitrogen adsorption data in the P/P_0 range from 0.05 to 0.30. Pore size distribution and total pore volume were calculated by the Gemini software using Barrett, Joyner, and Halenda (BJH) analysis for the adsorption data in the pore diameter range of 0.002 to 0.07 μm (14).

Moisture Uptake Studies

Moisture uptake by the granulations and MCC starting material was determined at 25°C using the Dynamic Vapor Sorption system (DVS-2, Surface Measurement Systems Ltd, Alpertown, UK). Moisture uptake by the sample, approximately 30 mg, was determined as the relative humidity was increased in increments of 5 or 10%. Equilibrium moisture uptake was determined by measuring weight gain at each relative humidity. Equilibrium was deemed to be achieved when the rate of weight change is less than 0.005% per minute.

Granulation Compactibility

Compaction profiles of the lubricated and unlubricated granulations and MCC starting material were obtained using ESH Tablet Compaction Simulator (Huxley Bertram Engineering, Cambridge, UK). A weight of 260 mg of each batch was compressed on the simulator using 3/8-in flat face tooling to a predetermined in-die thickness. Each batch was compressed to four different thickness targets with three tablets obtained at each thickness. Actual thickness achieved for each tablet compressed was determined by the linear variable displacement transducer (LVDT) of the compaction simulator. Compression force was also determined for each tablet using the upper punch strain gauge of the compaction simulator and converted to compression pressure. The hardness of each tablet was determined by diametral compression on a hardness tester (Key International) and converted to a tensile strength. Compaction profiles were then constructed using the compression pressure and corresponding compact tensile strength.

Two compaction parameters were also calculated from the compaction simulator data. The yield pressure was obtained from the slope of the linear portion of the natural logarithm of the reciprocal tablet porosity vs. compression pressure. A bonding parameter was calculated as the Y intercept of the plot of tensile strength vs. tablet porosity and represents theoretical tablet tensile strength at zero porosity.

Pore size distribution for tablets compressed using a compression force of 10 kN was also determined using the mercury intrusion porosimetry method described above. In addition to incremental pore volume (V), incremental pore wall surface area (A) was calculated using the equation $A = 4V/D$ for each increment (D is the mean pore diameter for the increment). Total pore volume and pore area were calculated for pore diameters ranging from 0.1 to 10 μm . The normalized pore wall surface area per unit pore volume was then calculated by dividing total pore area by pore volume for each tablet.

RESULTS AND DISCUSSION

Particle Size Measurements

Particle size measurements by mesh analysis and laser diffraction indicated minimal particle size growth for the undergranulated batch with HPC and the overgranulated batch without HPC (Table I). Geometric mean diameter determined by mesh analysis has only increased from 81 to 87 and 101 μm for the two batches, respectively. Similarly, laser diffraction data do not suggest an increase in particle size for the two batches compared to the starting material. On the other hand, the overgranulated batch with HPC showed significant increase in particle size compared to the starting material as indicated by the two particle size measurement techniques. Geometric mean diameter by mesh analysis was 214 μm and volume mean diameter by laser diffraction was 324 μm compared to 81 and 115 μm for the starting material determined by the two methods, respectively.

Ball milling of the two overgranulated batches seemed to reduce the particle size resulting in a smaller particle size than the starting material. Volume mean diameter by laser diffraction was 41 and 34 μm for the two ball-milled batches with and without HPC, respectively. The geometric mean particle size by mesh analysis was 54 and 89 μm for the two batches, respectively. The higher number for the ball-milled batch without HPC in this case is attributed to agglomeration

Table I. Physical Characterization of Granules and MCC Starting Material

	BET surface area (m^2/g)	BJH pore volume, 0.002–0.07 μm pore diameter (mL/g)	Geometric mean diameter by sieve analysis (μm)	Malvern particle size, volume mean diameter ($D[4,3]$, μm)	Mercury intrusion porosity (mL/g)		
					1–10 μm pore volume	0.1–1 μm pore volume	0.1–10 μm pore volume
MCC (starting material)	1.09	0.0032	81.3	114.9	0.4081 ^a	0.0791 ^a	0.4872 ^a
Undergranulated, HPC	0.91	0.0023	87	125.1	0.3639 ^a	0.0724 ^a	0.4364 ^a
Overgranulated, HPC	0.53	0.0013	214.3	324.1	0.0588 ^a	0.0461 ^a	0.1049 ^a
Overgranulated, HPC, ball milled	1.33	0.0060	53.9	41.4	0.4358	0.0481	0.4838
Overgranulated, no HPC	0.34	0.0008	101.1	97.6	0.1324 ^a	0.0398 ^a	0.1722 ^a
Overgranulated, no HPC, ball milled	1.24	0.0053	88.7	34.3	0.5431	0.0348	0.5779

^a 70- to 100-mesh fraction.

of the fine particles that would not break up during mesh analysis. The presence of agglomerates in this case was corroborated by visual observations.

Mercury Intrusion Porosimetry Studies

In a granulation process, primary particles of a starting material agglomerate to form larger aggregates described as granules. Three types of pores can hence exist in a granulated system: (1) void space between granules (intergranular pores), (2) pores between primary particles within the granules (intragranular pores), and (3) pores within the primary particles (intraparticulate pores).

Pore size distribution by MIP of a granulated system shows intergranular (void) space at lower pressures and intragranular/intraparticulate (pore) space at higher pressures. Void space is a function of particle size/packing and provides little useful information regarding pore structure. Intraparticulate/intragranular space, however, is directly related to pore structure and has been shown to correlate well with important particle performance characteristics such as compactibility (10,11).

MIP pore distribution profiles typically are bimodal or multimodal with the peaks at the larger pore sizes representing void space (Fig. 1A). In this study, 10 μm was taken as the cut-off point between pores and void space with values below 10 μm representing pores and values above 10 μm representing void space. To enhance resolution, samples were fractionated by sieve and the 70- to 100-mesh fraction was used for the MIP studies. Results for total pore volume in both the 0.1- to 1.0- and the 1.0- to 10.0- μm ranges are listed in Table I.

MCC starting material showed higher pore volume at all pore sizes than the granulated samples (Fig. 1B). Undergranulated material showed a modest decrease in porosity, whereas overgranulated material (with or without binder) showed a substantial decrease in porosity. Particle size in the overgranulated batch without the binder varies little from MCC indicating minimal granule growth. As a result, particles in the 70- to 100-mesh fraction are mainly primary MCC particles. The diminished porosity in this case is likely due to the decrease in pore volume between the smaller structures (15) within the MCC primary particles.

In the case of the overgranulated batch containing HPC, the significant particle growth suggests that particles in the 70- to 100-mesh range are a mixture of large primary particles and granulated small particles. Regardless of the origin of the particles, they seemed to have the lowest pore volume in the 0.1- to 10- μm range among all samples tested. In addition to the decrease in primary particle porosity, it can also be inferred that granules formed during processing of this batch are likely to possess low pore volume between the primary particles in the granule.

Ball milling of the overgranulated batches reduced particle size to such an extent that distinguishing between void space and pore structure became difficult in the 1.0- to 10.0- μm range. For this reason, evaluation of the porosity for the ball-milled batches was performed by examining pore volumes in the 0.1- to 1- μm range, which consists mainly of intragranular/intraparticulate pores. For both milled batches, pore volume in this range was similar to pore volume in the

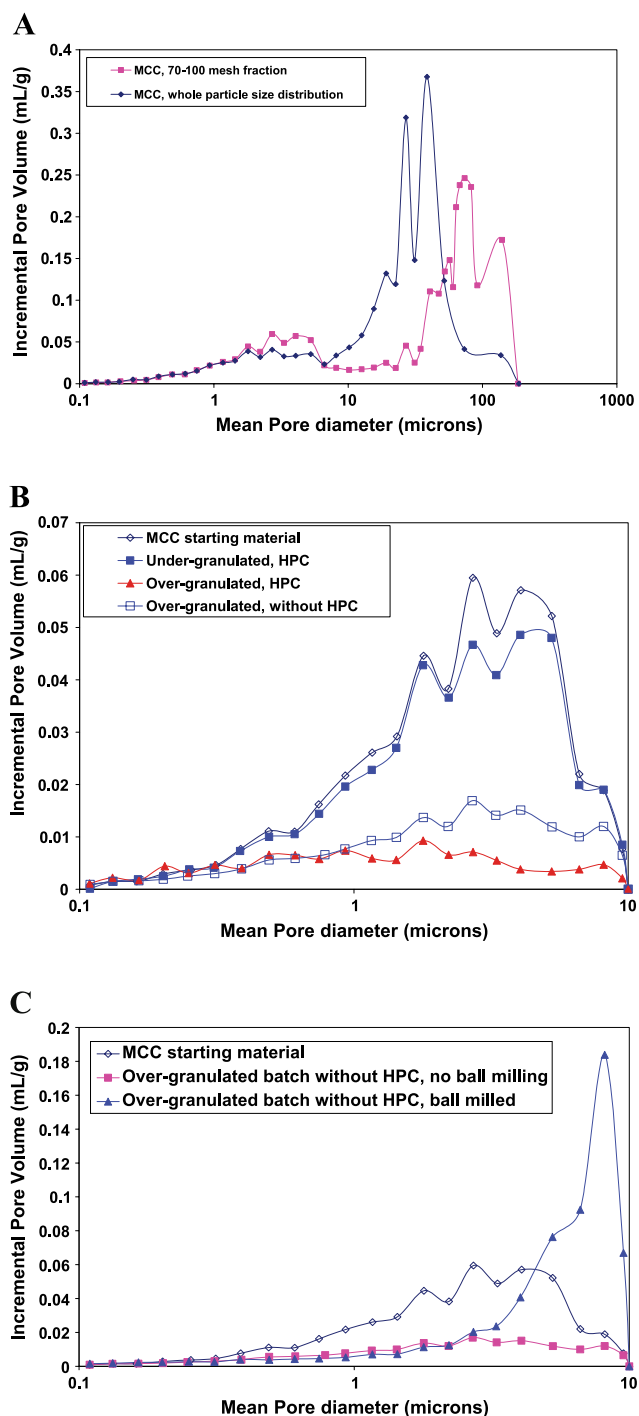


Fig. 1. Mercury intrusion pore size distribution of granulations of (A) MCC starting material, (B) granulation batches, and (C) ball-milled batch without HPC. Incremental intrusion volume represents pore volume associated with corresponding mean pore diameter.

unmilled samples, suggesting that ball milling does not affect the porosity in this pore size range (Fig. 1C).

Nitrogen Adsorption Studies

Granulation of MCC decreased its surface area in all cases (Table I). For the undergranulated HPC-containing batch, there was approximately 17% decrease in surface area

compared to ungranulated MCC. The decrease in surface area was even more pronounced for the overgranulated batches. Surface area reduction was approximately 51 and 69% for the overgranulated batches with and without HPC, respectively. The decrease in surface area seems to be more than expected from the increase in particle size alone, particularly for the overgranulated batch without HPC. Total surface area is the result of external surface area, which is inversely related to the particle size, and pore surface area within the particles or granules. Whereas minimal increase in particle size was observed for the overgranulated batch without HPC, its surface area was significantly lower than MCC and other granulated batches. Thus, it seems that the decrease in surface area in this case is primarily due to decrease in porosity. Ball milling increased the surface area of overgranulated batches and the surface area of milled materials was even slightly higher than ungranulated MCC.

Pore volume distribution was also obtained for pores in the 0.002- to 0.07- μm range from the nitrogen adsorption studies using BJH analysis (Table I). Due to the small pore size in this case, pore structure examined by this technique is almost exclusively limited to pores within the primary particle rather than pores between the primary particles in the granule structure. Similar to the 0.1- to 10- μm pore-diameter range examined by MIP, wet granulation also diminished pore volume in the 0.002- to 0.07- μm range. Significant reduction of the pore volume in the later range was observed for all granulated batches with more pronounced reduction observed for the two overgranulated batches. As stated above, the decrease in porosity resulting from wet granulation was reflected in the surface area reduction of the granulated batches, which seemed to be more pronounced than what would be expected from particle size enlargement alone.

Pore volume in the 0.002- to 0.07- μm range for the ball-milled material was substantially higher than the unmilled material from the same batch and higher than ungranulated MCC. This may be attributed to the formation of cracks or fissures during the ball-milling process. It is noteworthy that ball milling did not significantly change pore volume in the 0.1- to 1- μm range as determined by MIP, suggesting that any created cracks are mostly below 0.1 μm . The higher porosity of the ball-milled material in the 0.002- to 0.07- μm range is

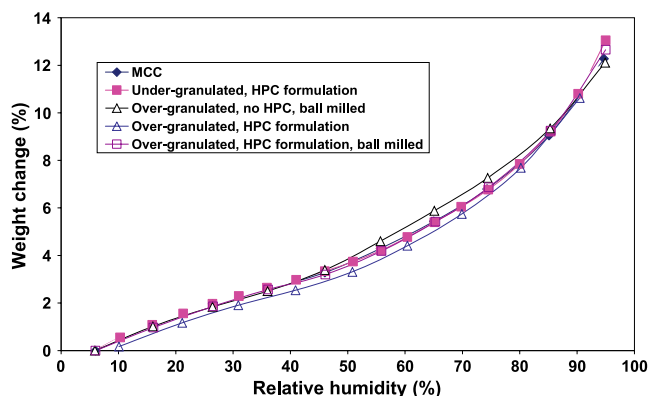


Fig. 2. Moisture uptake isotherms of granulations and of MCC starting material at 25°C.

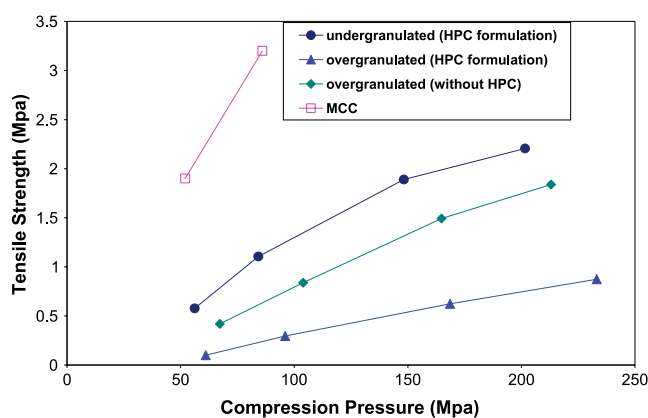


Fig. 3. Compaction profiles of un lubricated granulation and starting material.

likely to be a contributing factor to its higher surface area as described above.

Moisture Uptake Studies

Adsorption isotherms of the different granulations, starting material and ball-milled granulations were essentially identical (Fig. 2). Most of the moisture uptake by MCC and its processed formulations results from sorption by the amorphous regions of MCC (16). Water uptake by surface adsorption represents only a small fraction of the total moisture uptake by MCC, which explains the similar hygroscopicity of the different batches evaluated here despite their surface area differences. On the other hand, the similar moisture uptake of those formulations and the starting material suggests very little change in amorphous to crystalline ratio during processing.

Compaction Studies of Un lubricated Granulation

As expected, ungranulated MCC showed excellent compactibility. In all cases, granulated formulations were less compactible than MCC. Undergranulated HPC formulation showed higher compactibility than the same formulation processed using higher amount of water and more shear (overgranulated) (Fig. 3).

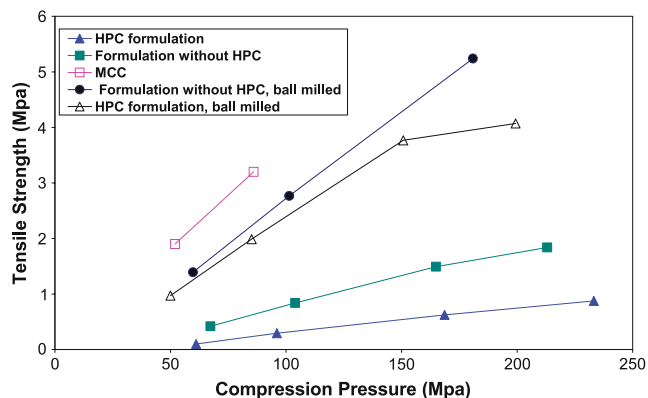


Fig. 4. Effect of milling on compactibility of overgranulated formulations.

Table II. Compaction Parameters for the Different Granulations and Starting Material

	Compactibility (kPa/MPa)	Yield pressure (MPa)	Bonding (MPa)
MCC (starting material)	41.03	72.84	5.42
Undergranulated, HPC	11.12	101.03	2.67
Undergranulated, HPC (lubricated)	9.31	106.51	2.16
Overgranulated, HPC	4.47	113.96	1.01
Overgranulated, HPC (lubricated)	0.60	133.45	0.13
Overgranulated, HPC, ball milled	21.54	92.11	4.94
Overgranulated, no HPC	9.85	107.09	2.27
Overgranulated, no HPC, ball milled	31.69	97.63	6.54

Overgranulated formulation without HPC showed higher compactibility than the overgranulated HPC formulation, which was manufactured using identical granulation parameters. The incorporation of HPC thus seemed to make the formulation more susceptible to reduction in compactibility when overgranulated, probably as it enhanced the growth of dense granules under those processing conditions. The overgranulated HPC-free formulation was still less compactible than MCC and the undergranulated HPC formulation. Ball milling of the two overgranulated formulations resulted in significant enhancement of compactibility approaching that of the ungranulated MCC (Fig. 4).

Wet granulation of MCC resulted in an increase in yield pressure and a decrease in bonding parameter calculated from the compaction simulator studies (Table II). The yield pressure is inversely related to the volume reduction propensity of the material; hence, an increase in yield pressure indicates lower tendency for plastic deformation or fragmentation. The bonding parameter is decreased if bond strength is decreased or if bonding surface area per unit volume is decreased. It is noteworthy that increase in fragmentation or plastic deformation can also contribute to enhanced bonding parameter by increasing bonding surface area in a given volume.

The increase in yield pressure upon wet granulation may be the result of the decrease in porosity observed for the wet granulated material. As described above, wet granulation seems to reduce MCC primary particle porosity. In addition, wet granulation process has also produced granules with lower porosity, particularly for the overgranulated batch with HPC. Dense less porous primary particles and/or granules

would be less prone to fragmentation or plastic deformation during compression, resulting in the observed increase in yield pressure.

The decrease in bonding parameter may be attributed to the decrease in bonding surface area per unit volume (bond volume density). This is supported by tablet pore size distribution, which showed the largest median pore diameter for the tablets compressed from the overgranulated HPC batch, followed by the undergranulated HPC batch and finally the ungranulated MCC (Fig. 5). A smaller pore diameter of a tablet is reflected in a higher pore surface area (hence higher bonding surface area) at a given porosity. Normalized pore area was 11.7, 8.9 and 5.2 m²/mL for the MCC, undergranulated and overgranulated batches, respectively. Decreased fragmentation or plastic deformation of the densified MCC particles/granules is a likely contributor to the observed decrease in pore surface area. It cannot be excluded, however, that the decrease in bonding parameter may also be due to reduced bond strength resulting from particle surface changes induced by wet granulation.

Ball milling of the overgranulated batches decreased their yield pressure compared to the unmilled material. The decrease in yield pressure was associated with the observed increase in pore volume in the 0.002- to 0.07- μ m pore diameter range. It is conceivable that cracks induced by the milling process may be the reason for the increase in porosity and the decrease in yield pressure. The presence of cracks would decrease particle strength, and hence reduce yield pressure. Ball milling also increased bonding parameter, which may be attributed to the increase in bonding surface area per unit volume resulting from the decrease in particle size.

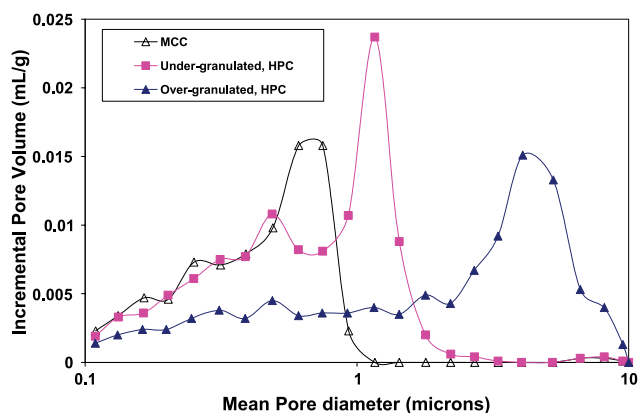


Fig. 5. Mercury intrusion pore size distribution of tablets obtained at 10 kN compression force.

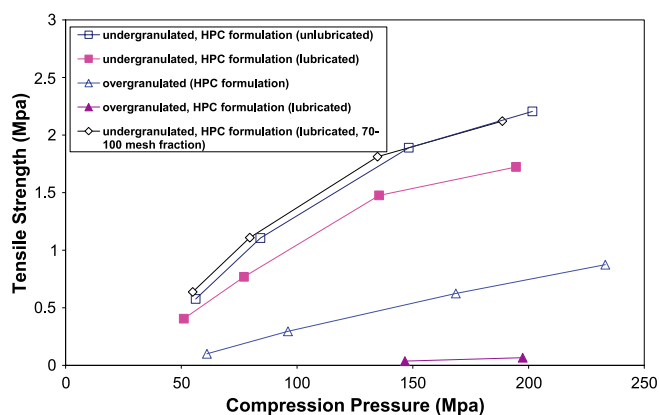


Fig. 6. Compaction profiles of the unlubricated and lubricated granulation batches.

Compaction Studies of Lubricated Granulation

Lubrication with magnesium stearate diminished compactibility of both under- and overgranulated batches containing HPC (Fig. 6). Compactibility reduction was more pronounced for the overgranulated compared to the undergranulated batch. Magnesium stearate is known to coat granules and particles, interferes with bond formation during compression and hence diminishes compactibility. Granule and primary particle fragmentation during compression exposes fresh surface, which are not coated with magnesium stearate, which will enhance bonding and compactibility. The more porous primary particles and granules from the undergranulated batch may have higher fragmentation tendency than the less porous material from the overgranulated batch and are hence less susceptible to the negative effect of magnesium stearate on compactibility.

Sieve fractions, 70–100 mesh, of the two lubricated granulations were also evaluated for compaction behavior. Compared to the whole granulation, compaction behavior of this large particle size fraction was different for the two batches. For the overgranulated batch, the 70- to 100-mesh fraction was less compactible than the whole granulation and intact tablets could not be obtained. On the contrary, the 70- to 100-mesh fraction of the undergranulated batch was more compactible than the whole granulation demonstrating a compaction profile similar to the unlubricated granulation. The difference in behavior between the two granulations may be explained by the different structure and fragmentation propensity of the 70- to 100-mesh particles for the two granulations. Due to the minimal particle growth during granulation, the larger particle size fraction of the undergranulated batch would consist mainly of large primary MCC particles. For this batch, the large primary particles seem to have higher fragmentation tendency than the smaller primary particles present in the whole granulation resulting in a higher lubricant sensitivity for the whole granulation. On the other hand, the large particle size fraction of the overgranulated batch contains a higher proportion of densified large granules. Those granules seem to have lower fragmentation tendency compared to the smaller primary particles and/or granules present in the whole granulation resulting in a higher lubricant sensitivity for the 70- to 100-mesh fraction.

CONCLUSIONS

The decrease in MCC compactibility by wet granulation was observed even without significant particle size growth and was associated with the decrease in MCC primary particle porosity. Aggregation of MCC particles into large dense granules when the binder is included in the formulation resulted in further decrease in compactibility.

Milling seems to counteract the effect of wet granulation on MCC compactibility where particle surface area and porosity are increased.

REFERENCES

1. J. N. Staniforth, A. R. Baichwal, J. P. Hart, and P. W. S. Heng. Effect of addition of water on the rheological and mechanical properties of microcrystalline cellulose. *Int. J. Pharm.* **41**: 231–236 (1988).
2. C. Gustafsson, H. Lennholm, T. Iversen, and C. Nystroem. Evaluation of surface and bulk characteristics of cellulose I powders in relation to compaction behavior and tablet properties. *Drug Dev. Ind. Pharm.* **29**(10):1095–1107 (2003).
3. G. Buckton, E. Yonemochi, W. L. Yoon, and A. C. Moffat. Water sorption and near IR spectroscopy to study the difference between microcrystalline cellulose before and after wet granulation. *Int. J. Pharm.* **181**:41–47 (1999).
4. Y. Nakai, S. Fukuoka, S. Nakajima, and K. Yamamoto. Crystallinity and physical characteristics of microcrystalline cellulose. II. Fine structure of ground microcrystalline cellulose. *Chem. Pharm. Bull.* **25**:2490–2496 (1977).
5. R. Huttenrauch. Identification of hydrogen bonds by means of deuterium exchange demonstration of binding forces in compressed cellulose forms. *Pharmazie* **26**:645–646 (1971).
6. G. P. Millili, R. J. Wigent, and J. B. Schwartz. Differences in mechanical strength of microcrystalline cellulose pellets are not due to significant changes in degree of hydrogen bonding. *Pharm. Dev. Technol.* **1**(3):239–249 (1996).
7. T. Suzuki, H. Kikuchi, S. Yamamura, K. Terada, and K. Yamamoto. Change in characteristics of microcrystalline cellulose during wet granulation using a high shear mixer. *J. Pharm. Pharmacol.* **53**:609–616 (2001).
8. P. Kleinebudde. The crystallite gel model for microcrystalline in wet granulation, extrusion and spheronization. *Pharm. Res.* **14**(6):804–809 (1997).
9. R. Ek and J. M. Newton. Microcrystalline cellulose as a sponge as an alternative concept to the crystallite gel model for extrusion and spheronization. *J. Pharm. Pharmacol.* **15**:509–510 (1998).
10. S. I. F. Badawy, M. M. Menning, M. A. Gorko, and D. L. Gilbert. Effect of process parameters on compressibility of granulation manufactured in a high shear mixer. *Int. J. Pharm.* **198**:51–56 (2000).
11. M. Wikberg and G. Alderborn. Compression characteristics of granulated materials. IV. The effect of granule porosity on the fragmentation propensity and compactibility of some granulations. *Int. J. Pharm.* **69**:239–253 (1991).
12. B. Johansson, M. Wickberg, R. Ek, and G. Alderborn. Compression behavior and compactibility of microcrystalline cellulose pellets in relation to their pore structure and mechanical properties. *Int. J. Pharm.* **117**:57–73 (1995).
13. S. Westermarck, A. M. Juppo, L. Kervinen, and J. Yliruusi. Microcrystalline cellulose and its microstructure in pharmaceutical processing. *Eur. J. Pharm. Biopharm.* **48**:199–206 (1999).
14. P. A. Webb and C. Orr. *Analytical Methods in Fine Particle Technology*. Micromeritics Instrument Corp., Norcross, GA, 1997, pp. 157, 80.
15. R. Ek, G. Alderborn, and C. Nystrom. Particle analysis of microcrystalline cellulose: differentiation between individual particles and their agglomerates. *Int. J. Pharm.* **111**:43–50 (1994).
16. G. Zografi and M. J. Kontny. The interaction of water with cellulose- and starch-derived pharmaceutical excipients. *Pharm. Res.* **3**:187–194 (1986).